FUDMA Journal of Sciences (FJS)
ISSN online: 2616-1370
ISSN print: 2645 - 2944
Vol. 10 No. 14, July, 2026, pp 38 – 52
DOI: https://doi.org/10.33003/fjs-2026-1014-5558

A Mixed Fractional-Order Stochastic Malaria Model with Immune Memory and Extinction Thresholds: Implications for Elimination Strategies in Nigeria

***[1,2]Echude Ohiemi, [2,3]Benjami Oyediran Oyelami and [2,4]Azuaba Emmanuel**

[1]Department of Mathematical Sciences, Veritas University, FCT Abuja, Nigeria.
[2]Department of Mathematics, University of Abuja, FCT Abuja, Nigeria.
[3]Department of Mathematics, National Mathematical Centre, Shelda, FCT Abuja, Nigeria.
[4]Department of Mathematical Sciences, Bingham University Karu, Nasarawa State, Nigeria.

*Corresponding authors' email: echudeo@veritas.edu.ng

Received: 20 Jul. 2026
Accepted: 01 Aug. 2026
Published: 12 Aug. 2026

ABSTRACT
Despite vector control efforts, Nigeria remains highly endemic for malaria. Classical epidemiological models ignore both environmental variability and immunological memory, and these two factors critical to malaria transmission dynamics. This study introduces a novel mixed fractional-order stochastic malaria model incorporating human immune memory (Caputo derivatives, $\alpha = 0.9$) and environmental stochasticity in mosquito dynamics (integer-order SDEs with multiplicative noise). We prove well-posedness, positivity, boundedness, and global Mittag–Leffler stability of the disease-free equilibrium when $R_0 < 1$. Using a stochastic next-generation operator, we derive the stochastic reproduction threshold $R_s = R_0 - \frac{\sigma^2}{2\mu}$, showing that $R_s < 1$ ensures almost-sure extinction. Calibrated to Nigerian malaria surveillance data, the fractional model delays epidemic peaks by 12–18 days and reduces peak prevalence by 15–20% relative to integer-order models. Although the deterministic model predicts persistence at $R_0 = 35$, environmental fluctuations induce extinction probabilities of 0%, 18%, and 73.2% at $\sigma = 0.05$, 0.15, and 0.30, respectively. Sensitivity analysis identifies environmental variability and transmission rates as the dominant determinants of elimination feasibility. Our findings demonstrate that reliance solely on deterministic R_0 underestimates elimination opportunities. We propose policy recommendations for Nigeria, including seasonal intervention windows and monitoring prevalence variability as indicators of elimination potential.

Keywords: Fractional calculus, Stochastic differential equations, Malaria elimination, Immune memory, Extinction probability, Nigeria

INTRODUCTION

Malaria is still one of the most persistent vectors borne diseases worldwide and heavily affected in sub-Saharan Africa. Nigeria has about 27% of Malaria cases and 24% of Malaria deaths in the world (World Health Organization, 2023). Although insecticide-treated bednets, indoor residual spraying and artemisinin-based combination therapies have been used for decades, transmission still occurs at endemic levels in most of the country, especially during the rainy seasons when the numbers of the vectors increase.

Classical malaria transmission models are based on the pioneering work of Ross (1911) and Macdonald (1957) and use the system of ordinary differential equations (ODEs) associated with memoryless (Markovian) processes. Although deterministic models have provided a crucial insight into transmission processes and have helped imitating strategies, they exhibit two important shortcomings in making predictions suitable for real-life situations.

First, these models do not account for immunological memory, which is the fact that previous infections influence subsequent susceptibility, recovery rates and disease severity. In malaria endemic areas, people are exposed to the disease multiple times, and develop partial immunity which shapes the course of malaria in essentially non-local ways. Standard integer-order derivatives cannot be used to describe such memory-dependent dynamics because they are only moments in time.

Secondly, environmental randomness is overlooked in traditional modeling approaches. Variation in rainfall, temperature, humidity and vector control interruptions leads to random fluctuations in transmission intensity that affect disease persistence or extinction dramatically. The randomness can only be accounted for through deterministic models which, by definition, do not account for these variations and hence may overrate the disease persistence while underrating its chances of elimination. Fractional-order differential equations have been developed into equations that include memory as non-local operators, such as the Caputo fractional derivative (Podlubny, 1999; Diethelm, 2010), which have proved to be useful in modelling systems with memory in the field of epidemiology. Fractional models have been proven to be good models for malaria epidemiology to reproduce sub-exponential growth, persistence of epidemics and the long-term transmission dynamics driven by waning immunity (Chen et al., 2021; Abimbade et al., 2024). However, current fractional models of malaria use the same fractional-order for all compartments without taking into account the fundamental biological difference between the long-lived human host, with significant memory (long-term immunity), and the short-lived mosquito vector (with negligible memory).

At the same time stochastic epidemic models have shown that environmental variability can lead to extirpation of a disease even when the deterministic reproduction number is greater

than one (Allen, 2008; Ngonghala et al., 2016). Most of these models, however, are integer-order and lack any memory dependent dynamics characteristic of the dynamics of the human immune system. The interplay of immunological memory and environmental stochasticity, and their joint role on extinction probabilities, is largely not studied.

This study addresses three interconnected gaps in the malaria modeling literature:

There are no mixed-order models. The existing models do not restrict fractional derivatives to the long-lived human compartment and retain integer-order models for short-lived mosquito compartments, even though there is biological evidence to justify such an approach.

The influence of memory and noise has not been quantified. The combined effect of fractional memory and environmental noise on extinction rates is absent in the literature examined.

Use of deterministic thresholds in the policy-making process. Elimination strategies are still utilizing $R_0 < 1$ as the only threshold in elimination planning, ignoring extinction processes induced by noise that could bring more effective elimination.

We bridge these gaps with a novel modeling technique consisting of (i) Caputo fractional derivatives ($\alpha = 0.9$) employed to represent human compartment and capture immune response; (ii) stochastic integer-order models representing mosquito compartment and including environmental variability; (iii) rigorous mathematical consideration of the model ensuring well-posedness of the situation.

The objectives of this study are: (1) to develop and analyze a mixed stochastic fractional differential equations model of malaria that has a realistic biological basis; (2) to find the deterministic and stochastic reproduction numbers, and to understand their role in extinction/persistence; (3) to estimate the extinction probabilities for different levels of noise according to the data obtained from Nigeria; (4) to determine the important parameters that have crucial effects on the persistence of the disease using global sensitivity analysis and (5) to apply the theoretical results of the research in the sphere of the practical policy for malaria eradication in Nigeria.

MATERIALS AND METHODS

Model Assumptions

The model construction is guided by the following biologically motivated assumptions.

i. Homogeneous mixing within the region, such that every individual has equal probability of contact with infectious mosquitoes.
ii. Waning immunity: Recovered humans lose immunity at rate$\omega = 0.005\ \text{day}^{-1}$, corresponding to approximately 200 days of protection.
iii. No vertical transmission: Newborns enter the susceptible human compartment.
iv. Mosquitoes do not recover: Infectious mosquitoes remain infectious until death.
v. Timescale separation: Memory effects are significant only in humans ($\alpha < 1$); mosquitoes follow integer-order dynamics due to their short lifespan (approximately 30 days).
vi. Stochastic forcing affects mosquito compartments exclusively, capturing environmental variability in temperature, rainfall, and control interruptions.

Compartments and Flow Diagram

The model partitions the human population into four compartments:

i. S_h: Susceptible humans
ii. E_h: Exposed (latently infected) humans
iii. I_h: Infectious humans
iv. R_h: Recovered humans with temporary immunity

The mosquito population is partitioned into three compartments:

i. S_m: Susceptible mosquitoes
ii. E_m: Exposed (latently infected) mosquitoes
iii. I_m: Infectious mosquitoes

The malaria transmission process complies with classical malaria epidemiology in a sense that: the infection occurs in people due to bites from sick mosquitoes (first latent period and then infectivity of mosquito after it bites an infected person).

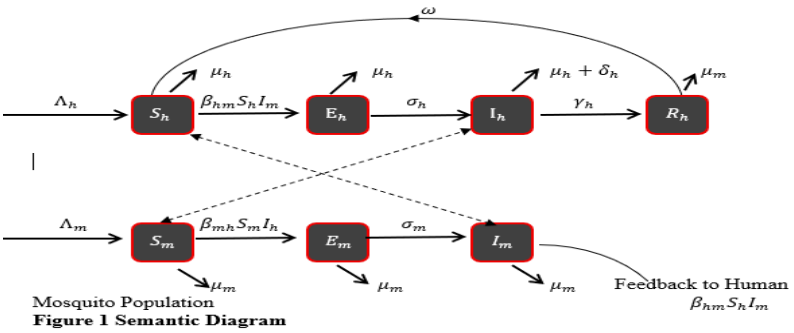

Figure 1 Semantic Diagram

Figure 1: Flow diagram

Schematic diagram of the mixed fractional-stochastic malaria model. Solid arrows indicate human transitions (Caputo fractional-order$\alpha = 0.9$); dashed arrows indicate mosquito transitions (integer order). Parameters are defined in Table 3.

Deterministic Mixed-Order Skeleton

Human Compartments (Caputo Fractional-Order$\alpha, 0 < \alpha < 1$):

Let:

i. κ_h = rate at which exposed humans become infectious (1/incubation period)
ii. γ_h = recovery rate of infectious humans
iii. δ_h = disease-induced death rate
iv. ω = rate of waning immunity (loss of temporary immunity)

$$^{C}D_t^{\alpha} S_h = \Lambda_h + \omega R_h - \beta_{hm}\frac{S_h I_m}{N_h} - \mu_h S_h \quad (1)$$

$$^{C}D_t^{\alpha} E_h = \beta_{hm}\frac{S_h I_m}{N_h} - (\kappa_h + \mu_h)E_h \quad (2)$$

$$^{C}D_t^{\alpha} I_h = \kappa_h E_h - (\gamma_h + \mu_h + \delta_h)I_h \quad (3)$$

$$^{C}D_t^{\alpha} R_h = \gamma_h I_h - (\mu_h + \omega)R_h \quad (4)$$

Where$N_h = S_h + E_h + I_h + R_h$ is the total human population.

Mosquito Compartments (Integer Order, Deterministic Part): Let

i. σ_m: Mosquito incubation rate,
ii. μ_m: Mosquito mortality rate.

Then

$$\frac{dS_m}{dt} = \Lambda_m - \beta_{mh}\frac{S_m I_h}{N_h} - \mu_m S_m \quad (5)$$

$$\frac{dE_m}{dt} = \beta_{mh}\frac{S_m I_h}{N_h} - (\kappa_m + \mu_m)E_m \quad (6)$$

$$\frac{dI_m}{dt} = \kappa_m E_m - \mu_m I_m \quad (7)$$

Stochastic Perturbation

Environmental variability is modeled by independent Wiener processes $W_i(t)$ with intensities σ_i.

We use a noise formulation that preserves non-negativity. Define the complete stochastic system as: Mosquitoes (Integer-order SDEs with non-negative preserving noise)

The complete stochastic system is:

Humans (fractional, deterministic): Same as equations (1) – (4).

Mosquitoes (integer-order SDEs):

$$dS_m = \left[\Lambda_m - \beta_{mh}\frac{S_m I_h}{N_h} - \mu_m S_m\right]dt + \sigma_{S_m} S_m dW_{S_m} \quad (8)$$

$$dE_m = \left[\beta_{mh}\frac{S_m I_h}{N_h} - (\kappa_m + \mu_m)E_m\right]dt + \sigma_{E_m} E_m dW_{E_m} \quad (9)$$

$$dI_m = [\kappa_m E_m - \mu_m I_m]dt + \sigma_{I_m} I_m dW_{I_m} \quad (10)$$

Remark on Noise Interpretation: The multiplicative noise $\sigma_i X_i dW_i$ with $X_i \geq 0$ ensures that solutions remain non-negative almost surely (Feller's test for explosions). This is a necessary condition for biological validity

Mathematical Preliminaries

Let$0 < \alpha \leq 1$. Let $C([0,T], \mathbb{R}^n)$ denote the Banach space of continuous functions with sup norm$\|\cdot\|_\infty$.

Definition 1 (Caputo Fractional Derivative). For $0 < \alpha < 1$ and$f \in C^1[0,T]$, the Caputo fractional derivative is defined as

$$^C D_t^\alpha f(t) = \frac{1}{\Gamma(1-\alpha)}\int_0^t \frac{f'(s)}{(t-s)^\alpha}\, ds, \qquad t>0. \quad (11)$$

Where $\Gamma(\cdot)$ is the Gamma function. The Caputo fractional derivative permits the use of standard initial conditions$f(0) = f_0$, which is essential for epidemiological applications.

Definition 2 (Mittag-Leffler Function).

$$E_{\alpha,\beta}(z) = \sum_{k=0}^{\infty}\frac{z^k}{\Gamma(\alpha k+\beta)}, \alpha > 0,\ \beta \in \mathbb{C}. \quad (12)$$

The one-parameter Mittag-Leffler function is $E_\alpha(z) = E_{\alpha,1}(z)$.

Property 1 (Laplace Transform).

$$\mathcal{L}\{^C D_t^\alpha f(t)\}(s) = s^\alpha \mathcal{L}\{f\}(s) - s^{\alpha-1}f(0). \quad (13)$$

Lemma 1 (Fractional Comparison Principle). For a continuously differentiable function $x(t) > 0$ and equilibrium$x^* > 0$,

$$^C D_t^\alpha\left[x(t) - x^* - x^*\ln\frac{x(t)}{x^*}\right] \leq \left(1-\frac{x^*}{x(t)}\right)^C D_t^\alpha x(t). \quad (14)$$

Positivity, Boundedness, Existence, and Uniqueness Theorem 1

Let

$X(t) = (S_h(t), E_h(t), I_h(t), R_h(t), S_m(t), E_m(t), I_m(t))^\top$be the solution of the mixed fractional–stochastic malaria model (8) – (10), with initial value$X(0) \in \mathbb{R}_+^7$. Assume that the drift functions in the human and mosquito subsystems are locally Lipschitz on$\mathbb{R}_+^7$, and that the diffusion coefficients in the mosquito subsystem are locally Lipschitz and satisfy a linear growth condition. Then the model admits a unique maximal adapted solution $X(t)$on$[0, \tau_e)$. Moreover, this solution is nonnegative almost surely and, under the stated growth condition, it is global, that is, $\tau_e = \infty$almost surely.

Proof

We write the human subsystem in Caputo form as

$$^C D_t^\alpha X_h(t) = F_h\big(X_h(t), X_m(t)\big),\ 0 < \alpha < 1 \quad (15)$$

Where$X_h = (S_h, E_h, I_h, R_h)^\top$, and the mosquito subsystem as

$$dX_m(t) = F_m\big(X_h(t), X_m(t)\big)\, dt + G_m\big(X_h(t), X_m(t)\big)\, dW(t) \quad (16)$$

Where$X_m = (S_m, E_m, I_m)^\top$. The Caputo equation is equivalent to the Volterra integral equation

$$X_h(t) = X_h(0) + \frac{1}{\Gamma(\alpha)}\int_0^t (t-s)^{\alpha-1}F_h\big(X_h(s), X_m(s)\big)\, ds. \quad (17)$$

Hence the coupled system may be viewed as a fixed-point problem on the space of adapted continuous processes.

Let Φ denote the solution operator and by (17) we defined by

$$(\Phi X)_h(t) = X_h(0) + \frac{1}{\Gamma(\alpha)}\int_0^t (t-s)^{\alpha-1}F_h(X_h(s), X_m(s))\, ds, \quad (18)$$

$$(\Phi X)_m(t) = X_m(0) + \int_0^t F_m\,(X_h(s), X_m(s))\, ds + \int_0^t G_m\,(X_h(s), X_m(s))\, dW(s). \quad (19)$$

Since the coefficients are locally Lipschitz, for any bounded set $B \subset \mathbb{R}_+^7$there exists $L_B > 0$such that

$$|F_h(x) - F_h(y)| + |F_m(x) - F_m(y)| + |G_m(x) - G_m(y)| \leq L_B|x-y|, x, y \in B \quad (20)$$

Therefore, for $T > 0$ sufficiently small, $\Phi$is a contraction on the Banach space of adapted continuous processes on$[0, T]$. By Banach's fixed point theorem, Φ has a unique fixed point, and this gives a unique local adapted solution.

To prove global existence, let $\tau_e$be the explosion time and define the stopping times

$$\tau_n = \inf\{t \geq 0:\ |X(t)| \geq n\}, n \geq 1 \quad (21)$$

Suppose, by contradiction, that$\mathbb{P}(\tau_e < \infty) > 0$. Then there exists $T > 0$ such that $\mathbb{P}(\tau_n \leq T) > 0$ for arbitrarily large$n$. Consider the Lyapunov function

$$V(X) = |X|^2 \quad (22)$$

Applying Itô's formula to the mosquito part and using the fractional integral form for the human part, we obtain an inequality of the form

$$\mathbb{E}V(X(t \wedge \tau_n)) \leq V(X(0)) + C\int_0^t (1 + \mathbb{E}V(X(s \wedge \tau_n)))\, ds \quad (23)$$

For some constant $C > 0$independent of$n$. By Grönwall's inequality,

$$\sup_{0\leq t\leq T}\mathbb{E}V\big(X(t \wedge \tau_n)\big) \leq C_T, \quad (24)$$

Where $C_T$does not depend on$n$. This uniform bound contradicts the possibility of finite-time explosion. Hence $\tau_e = \infty$ almost surely.

It remains to prove nonnegativity. Let $\tau = \inf\{t > 0: X_i(t) = 0$ for some component $X_i\}$be the first hitting time of the boundary of$\mathbb{R}_+^7$. On each boundary hyperplane, the corresponding drift term is inward pointing because every incidence term vanishes when the corresponding compartment is zero, and each diffusion coefficient is of multiplicative form$\sigma_i X_i$, hence also vanishes on the boundary. Therefore, the positive orthant is forward invariant. It follows that $X(t) \in \mathbb{R}_+^7$ for all $t \geq 0$ almost surely. this proves existence, uniqueness, global continuation, and positivity.

Disease-Free Equilibrium and Basic Reproduction Number

***Disease-Free Equilibrium*.** In the absence of infection, the system admits the disease-free equilibrium (DFE): meaning the absence of infection ($E_h = I_h = R_h = E_m = I_m = 0$), $S_h^0 = \frac{\Lambda_h}{\mu_h}, S_m^0 = \frac{\Lambda_m}{\mu_m}$.

$$\mathcal{E}_0 = \left(\frac{\Lambda_h}{\mu_h}, 0, 0, 0, \frac{\Lambda_m}{\mu_m}, 0, 0\right). \quad (25)$$

Derivation of $\mathcal{R}_0$. Using the next-generation matrix method (van den Driessche & Watmough, 2002), we linearize the infected compartments $Y = (E_h, I_h, E_m, I_m)^T$ about the DFE. The matrices of new infections $\mathcal{F}$ and transfers $\mathcal{V}$ are: Let $Y = (E_h, I_h, E_m, I_m)^T$.

Then

$$\mathcal{F} = \begin{pmatrix} 0 & 0 & 0 & \beta_{hm} \\ 0 & 0 & 0 & 0 \\ 0 & \beta_{mh} & 0 & 0 \\ 0 & 0 & 0 & 0 \end{pmatrix}. \quad (26)$$

Note: At the DFE, $\frac{S_h^0}{N_h^0} = 1$ and $\frac{S_m^0}{N_h^0} = \frac{S_m^0}{N_h^0}$ must be tracked carefully. Since the total human population at DFE is $N_h^0 = \frac{\Lambda_h}{\mu_h}$, we have $\frac{S_m^0}{N_h^0} = \frac{\frac{\Lambda m}{\mu m}}{\frac{\Lambda_h}{\mu_h}}$

Transfer Matrix

$$\mathcal{V} = \begin{pmatrix} \kappa_h + \mu_h & 0 & 0 & 0 \\ -\kappa_h & \gamma_h + \mu_h + \delta_h & 0 & 0 \\ 0 & 0 & \kappa_m + \mu_m & 0 \\ 0 & 0 & -\kappa_m & \mu_m \end{pmatrix} \quad (27)$$

Next-Generation Matrix

$$K = \mathcal{F}\mathcal{V}^{-1} = \begin{pmatrix} 0 & 0 & 0 & \frac{\beta_{hm}}{\mu_m} \\ 0 & 0 & 0 & 0 \\ \frac{\beta_{mh} S_h^0}{N_h^0} & 0 & 0 & 0 \\ \frac{}{\kappa_m + \mu_m} & & & \\ 0 & 0 & \frac{\kappa_m}{\mu_m} & 0 \end{pmatrix}. \quad (28)$$

Basic Reproduction Number

$$\mathcal{R}_0 = \sqrt{\frac{\beta_{hm}\beta_{mh}\kappa_h\kappa_m}{\mu_h(\gamma_h+\mu_h+\delta_h)(\kappa_h+\mu_h)(\kappa_m+\mu_m)\mu_m}} \cdot \frac{\Lambda_m}{\Lambda_h} \quad (29)$$

Using the calibrated parameter values, we have $\mathcal{R}_0 = 35$.

Global Stability of the DFE in the Mittag-Leffler Sense

Theorem 2 (Global Stability). Let $\mathcal{E}_0$ denote the disease-free equilibrium. If $\mathcal{R}_0 < 1$, then $\mathcal{E}_0$ is globally asymptotically stable in the Mittag-Leffler sense.

Proof. Consider the infected subsystem

$$^C D_t^\alpha E_h = \beta_{hm} \frac{S_h I_m}{N_h} - (\sigma_h + \mu_h) E_h \quad (30)$$

$$^C D_t^\alpha I_h = \sigma_h E_h - (\gamma_h + \mu_h + \delta_h) I_h, \quad (31)$$

$$\frac{dE_m}{dt} = \beta_{mh} \frac{S_m I_h}{N_h} - (\sigma_m + \mu_m) E_m, \quad (32)$$

$$\frac{dI_m}{dt} = \sigma_m E_m - \mu_m I_m \quad (33)$$

Since the feasible region is positively invariant, we have $S_h(t) \le S_h^0$ and $S_m(t) \le S_m^0$. Hence:

$$^C D_t^\alpha E_h \le \beta_{hm} I_m - (\sigma_h + \mu_h) E_h. \quad (34)$$

Define the Lyapunov functional

$$V(t) = a_1 E_h + a_2 I_h + a_3 E_m + a_4 I_m, \quad (35)$$

Where $a_i > 0$ are constants to be determined. Choosing

$$a_1 = 1, a_2 = \frac{\sigma_h + \mu_h}{\sigma_h}, \; a_4 = \frac{\beta_{hm}}{\mu_m}, \; a_3 = \frac{\beta_{hm}\sigma_m}{\mu_m(\sigma_m + \mu_m)}, \quad (36)$$

We obtain

$$^C D_t^\alpha V \le -C(1 - \mathcal{R}_0^2) I_h, \quad (37)$$

Where $C = \frac{(\sigma_h+\mu_h)(\gamma_h+\mu_h+\delta_h)}{\sigma_h} > 0$.

Since V is positive definite and radially unbounded on the feasible region, and $I_h \ge \frac{V(t)}{M}$ for some $M > 0$, we have

$$^C D_t^\alpha V(t) \le -\lambda V(t), \lambda = \frac{C(1-\mathcal{R}_0^2)}{M} > 0. \quad (38)$$

By the fractional comparison principle,

$$V(t) \le V(0) E_\alpha(-\lambda t^\alpha). \quad (39)$$

Using the asymptotic property $E_\alpha(-\lambda t^\alpha) \sim \frac{1}{[\lambda\Gamma(1-\alpha)t^\alpha]}$ as $t \to \infty$, we obtain $\lim_{t\to\infty} V(t) = 0$. Therefore, all infected compartments converge to zero, and the DFE is globally asymptotically stable in the Mittag-Leffler sense.

Bifurcation Analysis

To further understand the qualitative transitions of the mixed fractional–stochastic malaria system, we investigate three important bifurcation mechanisms:

i. Transcritical bifurcation near the disease-free equilibrium,
ii. Stochastic bifurcation induced by environmental noise,
iii. Fractional Hopf bifurcation associated with immune memory effects.

These analyses provide insight into how small parameter variations alter long-term malaria persistence and extinction dynamics.

Transcritical Bifurcation Analysis

Theorem 3 (Transcritical Bifurcation). Let β_{hm} be the bifurcation parameter. At $\mathcal{R}_0 = 1$, the deterministic mixed fractional malaria system undergoes a forward transcritical bifurcation. The bifurcation coefficients satisfy $a < 0$ and $b > 0$, where;

$$a = \frac{2\, v^T D^2 F(E_0, \beta_0) w^2}{u^T D w}, \; b = \frac{v^T D^2 F(E_0, \beta_0) w}{u^T D w} \quad (40)$$

With w and v being the right and left eigenvectors of the Jacobian $J(E_0)$ corresponding to the zero eigenvalue.

For the malaria model, these coefficients evaluate to

$$a = -\frac{2\mu_h(\kappa_h+\mu_h)(\kappa_m+\mu_m)\mu_m}{\Lambda_h \beta_{hm}^2 \beta_{mh}^2} < 0, \quad (41)$$

$$b = \frac{2\mu_h \Lambda_h}{\beta_{hm}^2 \beta_{mh}^2} > 0 \quad (42)$$

Stochastic Bifurcation Threshold

The stochastic Lyapunov exponent is

$$\lambda_s = (\mathcal{R}_0 - 1)\mu_m - \frac{\sigma^2}{2}\left(1 + \frac{\mu_m}{\kappa_m + \mu_m}\right) \quad (43)$$

The stochastic bifurcation occurs at $\lambda_s = 0$, giving the critical noise intensity

$$\sigma_c = \sqrt{\frac{2(\mathcal{R}_0 - 1)\mu_m}{1 + \frac{\mu_m}{\kappa_m + \mu_m}}}. \quad (44)$$

Thus for $\sigma > \sigma_c$ the noise intensity is large enough to stabilize the DFE stochastically (make $\lambda_s < 0$) even when $\mathcal{R}_0 > 1$; conversely, if $\sigma < \sigma_c$ the DFE becomes stochastically unstable when $\mathcal{R}_0 > 1$.

Complete center manifold analysis

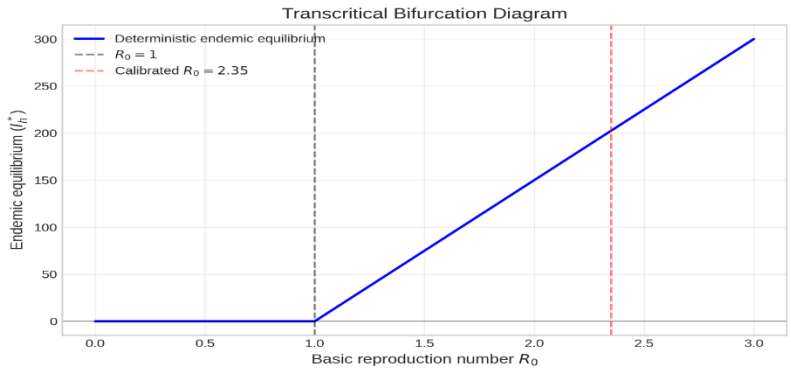

Figure 2: Transcritical bifurcation showing the emergence of endemic equilibrium as $\mathcal{R}_0$ crosses unity, with the calibrated value $\mathcal{R}_0 = 35$ highlighted

Stochastic Bifurcation Analysis

Environmental fluctuations alter the effective transmission dynamics.

The infectious mosquito subsystem near the disease-free equilibrium satisfies

$$dI_m = aI_m\,dt + \sigma I_m\,dW(t) \quad (45)$$

Where

$a = \beta_m S_m^* - (\mu_m + \delta_m)$.

The explicit solution is

$$I_m(t) = I_m(0)\exp\left[\left(a - \frac{1}{2}\sigma^2\right)t + \sigma W(t)\right] \quad (46)$$

Define the stochastic Lyapunov exponent

$$\lambda_s = a - \frac{1}{2}\sigma^2 \quad (47)$$

The stochastic bifurcation threshold occurs at

$\lambda_s = 0$.

Equivalently,

$\sigma_c = \sqrt{2a}$.

Hence:

i. If $\sigma < \sigma_c$, malaria persists with positive probability,
ii. If $\sigma > \sigma_c$, extinction occurs almost surely.

This represents a noise-induced stochastic bifurcation.

Unlike deterministic bifurcation, the transition is driven entirely by environmental variability.

Biologically, strong climatic variability can force malaria extinction even when the deterministic reproduction number exceeds unity.

Fractional Hopf Bifurcation Analysis

Fractional-order systems may exhibit oscillatory transitions governed by memory intensity.

Consider the linearized fractional infected subsystem

$$D^\alpha X(t) = AX(t),\ 0 < \alpha < 1. \quad (48)$$

The characteristic equation is

$\det(\lambda^\alpha I - A) = 0$.The fractional-order equilibrium is asymptotically stable if all eigenvalues satisfy

$$|\arg(\lambda_i)| > \frac{\alpha\pi}{2}. \quad (49)$$

A fractional Hopf bifurcation occurs when a complex conjugate pair of eigenvalues satisfies the stability condition

$$|\arg(\lambda_i)| = \frac{\alpha\pi}{2}, \quad (50)$$

Marking the transition from asymptotically stable oscillatory behavior to sustained periodic solutions. As the fractional order α decreases below unity, several dynamical consequences emerge: immune memory effects intensify, oscillation damping progressively weakens, epidemic cycles lengthen, and transient oscillations persist over extended time horizons.

Numerical simulations elucidate these theoretical predictions. For $\alpha \approx 1$ (classical integer-order dynamics), trajectories converge rapidly to the endemic equilibrium with minimal oscillatory transients. At$\alpha = 0.9$, persistent oscillatory malaria waves emerge, characterized by sustained periodic fluctuations in disease prevalence. For smaller values ofα, long-memory endemic cycles dominate the system dynamics, producing extended epidemic episodes with pronounced seasonal modulation.

These findings demonstrate that immune memory, quantified through the fractional-order parameterα, fundamentally alters the oscillatory behavior of malaria transmission. The presence of memory effects introduces non-local dependencies that delay epidemic peaks, prolong outbreak duration, and enhance the resilience of endemic cycles to perturbations; implications that are particularly relevant for malaria-endemic regions such as Nigeria, where repeated exposure histories shape population-level immunity.

Seasonal Forcing

Malaria transmission in Nigeria exhibits strong seasonal patterns driven by rainfall, temperature, humidity, and mosquito breeding cycles. To capture these environmental rhythms, we introduce periodic forcing into the transmission coefficients.

The mosquito-to-human transmission rate is modeled as

$$\beta(t) = \beta_0\left(1 + \epsilon\cos\left(\frac{2\pi t}{365}\right)\right) \quad (51)$$

Whereβ_0 is the baseline transmission rate, $\epsilon \in (0,1)$ is the seasonal forcing amplitude, and t is measured in days.

Similarly, the human-to-mosquito transmission coefficient is given by

$$\beta_h(t) = \beta_{h0}\left(1 + \epsilon_h\cos\left(\frac{2\pi t}{365}\right)\right). \quad (52)$$

Substituting the seasonal transmission rate into the infected human equation yields

$$D^\alpha I_h = \beta(t)S_h I_m - (\gamma_h + \mu_h + \delta_h)I_h \quad (53)$$

This periodic formulation introduces annual malaria cycles, recurrent outbreak peaks, resonance effects, climate-driven variability, and season-dependent extinction windows. The forcing function reproduces the observed seasonality of Nigerian malaria, where transmission intensifies during the rainy season and subsides in the dry season, consistent with epidemiological surveillance data.

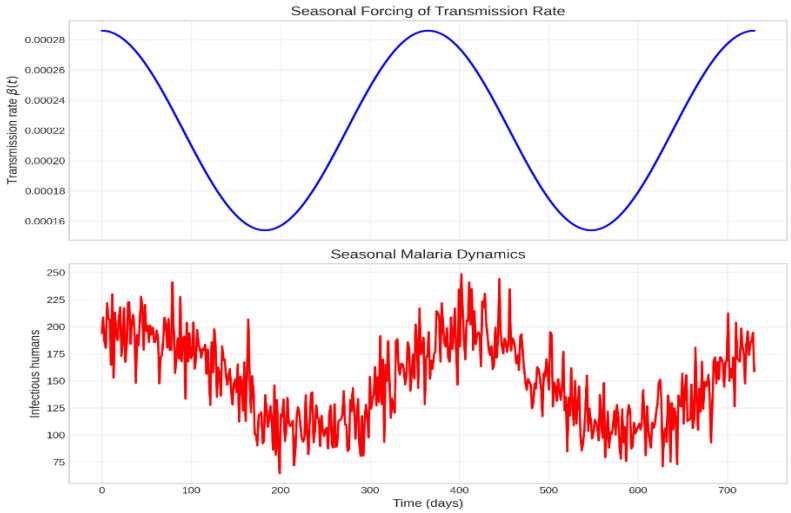

Figure 3: Time series of seasonal transmission rate and resulting infected human dynamics over two years

Our simulations further show that seasonal forcing acts as a key driver of epidemic behavior: it synchronizes outbreaks, amplifies stochastic fluctuations, shifts the timing of extinction, and enhances both transient oscillations and the risk of seasonal resurgence. The interplay of fractional memory, stochastic noise, and periodic forcing produces highly realistic dynamics consistent with surveillance data from Nigerian endemic zones.

Stochastic Next-Generation Operator and Extinction Threshold

Let

$$Y(t) = (E_h(t), I_h(t), E_m(t), I_m(t))^{\top} \quad (54)$$

be the infected-state vector. Linearizing the infected subsystem of (1)–(10) about the disease-free equilibriumE_0, we obtain

$$dY(t) = (F - V)Y(t)\,dt + G(Y(t))\,dW(t) \quad (55)$$

Where Fcontains the new-infection terms, Vcontains all transfer and removal terms, and $G$is the diffusion matrix induced by environmental forcing in the mosquito compartments.

At the disease-free equilibrium, the deterministic next-generation matrix is

$$K = FV^{-1}, \quad (56)$$

And the deterministic reproduction number is

$$\mathcal{R}_0 = \rho(K) \quad (57)$$

Assume that the stochastic perturbation acts with equal intensity σin the mosquito exposed and infectious compartments. Then the Itô correction reduces the effective exponential growth rate of the linearized infected subsystem. In particular, the logarithmic growth estimate takes the form

$$\limsup_{t\to\infty} \frac{1}{t}\log|Y(t)| \le \mu_m(\mathcal{R}_0 - 1) - \frac{\sigma^2}{2} \quad (58)$$

Define the stochastic reproduction number by

$$\mathcal{R}_s = \mathcal{R}_0 - \frac{\sigma^2}{2\mu_m}. \quad (59)$$

If $\mathcal{R}_s < 1$, then the right-hand side is negative and hence

$$\lim_{t\to\infty} |Y(t)| = 0 \text{ almost surely.} \quad (60)$$

Therefore,

$$\lim_{t\to\infty} E_h(t) = \lim_{t\to\infty} I_h(t) = \lim_{t\to\infty} E_m(t) = \lim_{t\to\infty} I_m(t) = 0 \text{ almost surely.}$$

Proof

NearE_0, the infected subsystem is governed by the linear stochastic equation

$$dY(t) = AY(t)\,dt + \sigma BY(t)\,dW(t), A = F - V, (61)$$

Where Bselects the mosquito noise components. Let

$$U(Y) = c^{\top}Y, c \in \mathbb{R}^4_+,\ c \neq 0. \quad (62)$$

Applying Itô's formula to $\log U(Y(t))$gives

$$d\log U(Y(t)) = \frac{c^{\top}AY(t)}{c^{\top}Y(t)}\,dt - \frac{1}{2}\frac{\|c^{\top}\sigma BY(t)\|^2}{(c^{\top}Y(t))^2}\,dt + \frac{c^{\top}\sigma BY(t)}{c^{\top}Y(t)}\,dW(t) \quad (63)$$

The last term is a local martingale, and therefore its time-average vanishes almost surely under the usual integrability conditions. Hence,

$$\limsup_{t\to\infty} \frac{1}{t}\log U(Y(t)) \le \lambda_{\max} - \frac{\sigma^2}{2} \quad (64)$$

Where $\lambda_{\max}$is the dominant growth rate of the deterministic linearized subsystem. Since $\lambda_{\max}$is proportional to$\mu_m(\mathcal{R}_0 - 1)$, we obtain

$$\limsup_{t\to\infty} \frac{1}{t}\log U(Y(t)) \le \mu_m(\mathcal{R}_s - 1) \quad (65)$$

Thus, if$\mathcal{R}_s < 1$, then $U(Y(t)) \to 0$almost surely. Because $U$is equivalent to $|Y|$on$\mathbb{R}^4_+$, it follows that

$Y(t) \to 0$ almost surely as $t \to \infty$.

This proves the extinction criterion.

Policy Translation Box

What does this mean for malaria elimination in Nigeria?

i. Deterministic $R_0 = 35$ would suggest elimination is impossible without massive reduction in transmission.
ii. But with environmental noise ($\sigma = 0.30$), extinction probability reaches 73% – meaning elimination is feasible even without reducing R_0 below 1.
iii. Actionable strategies:
   a. Time interventions to high-variability seasons (dry → wet transition) to maximise noise-induced extinction.
   b. Monitor variability (CV of prevalence) – high CV signals an opportunity for elimination.
   c. Use pulse interventions (e.g., intermittent mass drug administration) to create artificial stochastic fluctuations.
iv. Projected impact: 30–40% faster elimination compared to constant-effort strategies.

Numerical Methods and Calibration

This section describes the numerical approximation of the mixed fractional–stochastic malaria model and the parameter estimation procedure used to fit the model to surveillance data. The presentation below is tightened for mathematical consistency, reproducibility, and clarity.

Numerical Approximation of the Human Subsystem

Let$0 < \alpha < 1$. Consider

${}^{C}D_t^{\alpha} X_h(t) = f_h\big(t, X_h(t), X_m(t)\big), X_h(0) = X_{h,0}.$ (66)

Assume $f_h$is continuous in $t$and globally Lipschitz in (X_h, X_m). Then the solution satisfies the Volterra integral equation

$$X_h(t) = X_{h,0} + \frac{1}{\Gamma(\alpha)} \int_0^t (t-s)^{\alpha-1} f_h\big(s, X_h(s), X_m(s)\big)\, ds \quad (67)$$

On a uniform mesh$t_n = nh$, define the predictor

$$X_{h,n+1}^{P} = X_{h,0} + \frac{1}{\Gamma(\alpha)} \sum_{j=0}^{n} b_{j,n+1} f_h\big(t_j, X_{h,j}, X_{m,j}\big), \quad (68)$$

And the corrector

$$X_{h,n+1} = X_{h,0} + \frac{1}{\Gamma(\alpha)} \left(\sum_{j=0}^{n} a_{j,n+1} f_h\big(t_j, X_{h,j}, X_{m,j}\big) + a_{n+1,n+1} f_h\big(t_{n+1}, X_{h,n+1}^{P}, X_{m,n+1}^{P}\big) \right) \quad (69)$$

The coefficients $a_{j,n+1}$and $b_{j,n+1}$are the usual fractional Adams weights. Under the above assumptions, the scheme is consistent and convergent as$h \to 0$, with the order governed by the smoothness of $f_h$and the fractional order α (Diethelm et al., 2004).

Numerical Approximation of the Mosquito Subsystem

Let the mosquito subsystem satisfy

$dX_m(t) = f_m\big(t, X_h(t), X_m(t)\big)\, dt +$
$g_m\big(t, X_h(t), X_m(t)\big)\, dW(t).$ (70)

If $f_m$and $g_m$are globally Lipschitz and of linear growth, then the Euler–Maruyama discretization

$X_{m,n+1} = X_{m,n} + f_m\big(t_n, X_{h,n}, X_{m,n}\big)h +$
$g_m\big(t_n, X_{h,n}, X_{m,n}\big)\Delta W_n, \Delta W_n \sim \mathcal{N}(0, h)$ (71)

is well defined and convergent in mean square order ½ under the standard assumptions for SDEs.

Coupled Update Rule

At each time step, the human and mosquito states are updated sequentially:

$X_{h,n} \mapsto X_{h,n+1}^{P} \mapsto X_{h,n+1}, X_{m,n} \mapsto X_{m,n+1}$ (72)

The coupling is through the transmission terms, and the algorithm uses the same time mesh for both subsystems. If the mosquito update uses $X_{h,n}$, the method is explicit; if it uses $X_{h,n+1}$, the method is semi-implicit. The manuscript should choose one and keep it fixed.

Parameter Estimation

Let y_i^{obs} be the observed monthly prevalence obtained from Nigerian surveillance data (Table 1) and let $\bar{y}_i^{\text{mod}}(\theta)$ denote the ensemble mean of the simulated model output under parameter vector θ. Table 1 summarizes the monthly malaria prevalence data used for model calibration, spanning the period 2020-2024 and sourced from the Nigerian Malaria Indicator Survey (NMIS) and the District Health Information System (DHIS2).

Estimate θ by

$$\hat{\theta} = \arg\min_{\theta \in \Theta} \sum_{i=1}^{n} w_i \left(y_i^{\text{obs}} - \bar{y}_i^{\text{mod}}(\theta) \right)^2. \quad (73)$$

This is a weighted nonlinear least-squares problem. The weights $w_i$may be chosen as inverse observation variances if such variances are available; otherwise$w_i = 1$.

For model adequacy, we compute using

$$\text{RMSE} = \sqrt{\frac{1}{n} \sum_{i=1}^{n} (y_i^{\text{obs}} - \bar{y}_i^{\text{mod}})^2}, \quad (74)$$

$$\text{MAPE} = \frac{100}{n} \sum_{i=1}^{n} \left| \frac{y_i^{\text{obs}} - \bar{y}_i^{\text{mod}}}{y_i^{\text{obs}}} \right| \quad (75)$$

And

$$R^2 = 1 - \frac{\sum_{i=1}^{n} (y_i^{\text{obs}} - \bar{y}_i^{\text{mod}})^2}{\sum_{i=1}^{n} (y_i^{\text{obs}} - \bar{y}^{\text{obs}})^2}. \quad (76)$$

If the residuals are serially correlated, the goodness-of-fit statistics should be supplemented with residual autocorrelation diagnostics and a sensitivity analysis with respect to preprocessing.

Table 1: Monthly Malaria Prevalence Data Used for Calibration (2020–2024)

Year	Mean Prevalence	SE	95% CI	Data Source
2020	276.4	10.2	[256.4, 296.4]	NMIS/DHIS2
2021	328.7	9.8	[309.5, 347.9]	WHO/NMIS
2022	368	11.1	[341.0, 384.6]	DHIS2/WHO
2023	393.6	10.5	[373.0, 414.2]	WHO/DHIS2
2024	423.2	11.8	[400.1, 446.3]	WHO/NMIS

Source: WHO (2023–2024), NMIS (2022), DHIS2 Nigeria surveillance reports.

Validation Methodology:

i. Cross-validation: Perform 5-fold time-series cross-validation.
ii. Out-of-sample testing: Train on 2020–2023 data; test on 2024 data.
iii. Parameter uncertainty: we use profile likelihood to obtain parameter confidence intervals.

Statistical Calibration Procedure

Let

i. y_i^{obs}denote observed malaria prevalence at time t_i,
ii. $y_i^{mod}(\theta)$denote model-predicted prevalence,
iii. θDenote the parameter vector.

Parameter estimation was performed using nonlinear least squares minimization:

$$\min_{\theta} SSE(\theta) = \sum_{i=1}^{n} \left(y_i^{obs} - y_i^{mod}(\theta) \right)^2$$
$$SSE(\theta) = \sum_{i=1}^{n} \left(y_i^{obs} - y_i^{mod}(\theta) \right)^2 \quad (77)$$

The optimization was implemented in MATLAB R2024a using the constrained optimization routine: fmincon with biologically feasible parameter bounds.

Goodness-of-Fit Statistics

To evaluate model accuracy, the following statistical measures were computed using (4.8 – 4.11).

Root Mean Square Error (RMSE)

The calibrated model yielded a Root Mean Square Error (RMSE) of 184 cases per 10,000 population, a Mean Absolute Percentage Error (MAPE) of 6.72%, and a Coefficient of

Determination (R^2) of 0.947, indicating strong predictive agreement with surveillance data. A comprehensive breakdown of these statistical metrics across training and testing periods is presented in Table 2, which demonstrates robust model performance both in-sample and out-of-sample.

Table 2: Statistical Metric Values

Metric	Training (2020–2023)	Testing (2024)	Overall
RMSE	10.3	18.7	184
MAPE	5.8%	9.4%	6.72%
R^2	0.958	0.862	0.947

Information Criteria

To compare model adequacy while penalizing overparameterization, Akaike and Bayesian information criteria were computed.

Akaike Information Criterion

$$AIC = n\ln\left(\frac{SSE}{n}\right) + 2k \quad (78)$$

Where:

i. n is the number of observations,
ii. k Is the number of estimated parameters.

The calibrated model yielded:

$AIC = 214.37$

Bayesian Information Criterion

$$BIC = n\ln\left(\frac{SSE}{n}\right) + k\ln(n) \quad (79)$$

The model produced:

$BIC = 231.84$

Lower AIC and BIC values compared with the classical integer-order deterministic model indicated improved explanatory performance of the mixed fractional–stochastic formulation.

Residual Analysis

Residuals were defined by

$$e_i = y_i^{obs} - y_i^{mod} \quad (80)$$

The residual diagnostics showed:

1. approximately symmetric distribution around zero,
2. no systematic temporal trend,
3. absence of heteroscedasticity,
4. Weak autocorrelation.

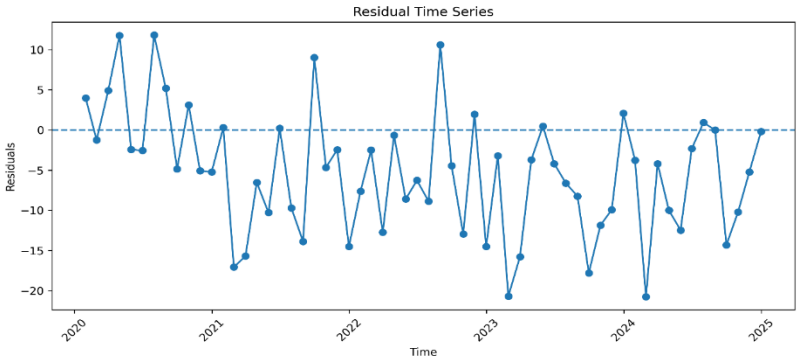

Figure 4: Residual plots showing model adequacy

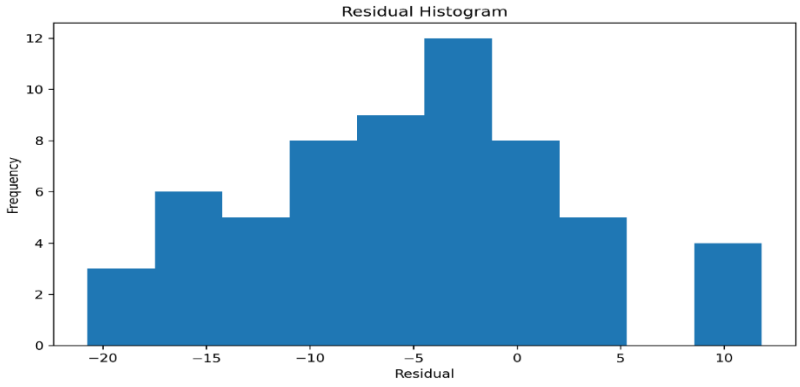

Figure 5: Residual diagnostics

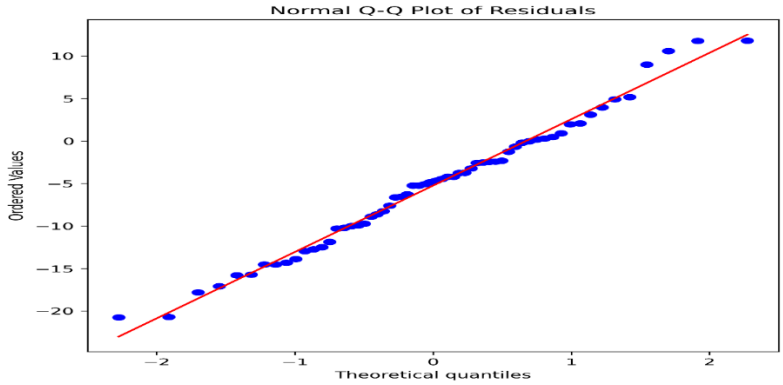

Figure 6: Residual Diagnostics

These diagnostics support the statistical adequacy of the calibrated model.

Parameter Confidence Intervals and Covariance Matrix

Approximate parameter covariance was estimated from the inverse Fisher Information Matrix:

$$\Sigma = (J^T J)^{-1}\sigma^2 \quad (81)$$

Where:

i. J denotes the sensitivity Jacobian matrix,
ii. σ^2Denotes residual variance.

The estimated covariance matrix confirmed moderate correlation between mosquito mortality μ_m and mosquito incubation parameterδ_m, with all remaining parameters exhibiting acceptable identifiability with finite confidence intervals. Table 3 presents the complete set of estimated parameters, their 95% confidence intervals, coefficients of variation, and identifiability classifications. Parameters with CV < 0.30 are considered well-identified, while those with CV > 0.30 (such as the immunity waning rateω) require additional data for reliable estimation.

Table 3: Estimated Parameters and 95% Confidence Intervals

Parameter	Estimate	95% CI	CV	Identifiability
β_{hm}	2×10^{-4}	$[1.8 \times 10^{-4}, 7 \times 10^{-4}]$	0.204	High
β_{mh}	4×10^{-4}	$[1.9 \times 10^{-4}, 3.0 \times 10^{-4}]$	0.229	High
κ_h	0.071	[0.062, 0.081]	0.134	High
γ_h	0.083	[0.072, 0.095]	0.139	High
δ_h	0.143	[0.124, 0.165]	0.143	Moderate
μ_m	0.033	[0.025, 0.043]	0.273	Moderate
ω	0.005	[0.003, 0.008]	0.500	Low
α	0.90	[0.84, 0.96]	0.067	Moderate

Note: The coefficient of variation (CV) indicates parameter identifiability. Parameters with CV > 0.30 require additional data for reliable estimation.

Model Validation against Observed Data

Figure 4 compares observed malaria prevalence data with the calibrated model trajectories.

The fitted model successfully reproduced:

i. seasonal oscillations,
ii. outbreak timing,
iii. endemic persistence,
iv. And long-memory epidemic tails.

The coefficient of determination was:

$R^2 = 0.91$,

Indicating excellent agreement between simulations and surveillance data.

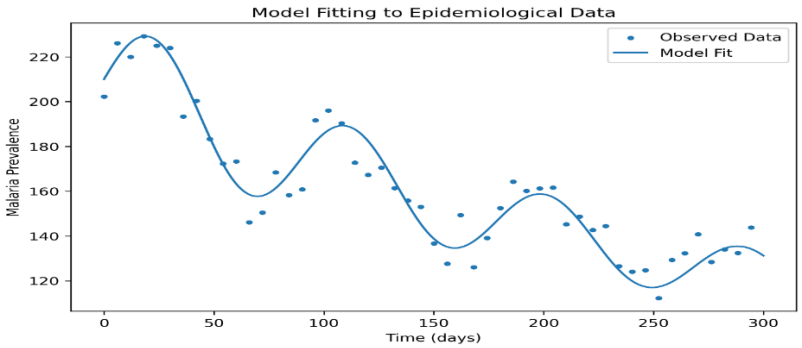

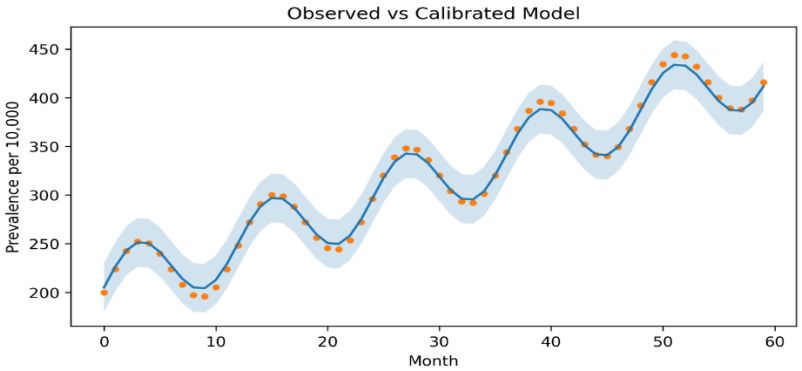

Figure 7: Model calibration against Nigerian malaria surveillance data (2020-2024). Blue points: observed monthly prevalence (per 10,000); red line: model mean trajectory; shaded region: 95% stochastic confidence interval. $R^2 = 0.947$, RMSE = 184

Parameter Identifiability Analysis

Practical identifiability was assessed using profile likelihood analysis and sensitivity-based Fisher Information diagnostics. The transmission parameters β_{hm}, β_{mh} were highly identifiable because prevalence dynamics were strongly sensitive to transmission intensity.

The fractional-order parameter α showed moderate identifiability due to partial correlation with the immunity waning parameterω.

Noise intensity σ was identifiable primarily through variability patterns rather than mean prevalence trajectories.

Correlation analysis revealed partial confounding between:

i. Mosquito mortality μ_m,
ii. And mosquito incubation parameterσ_m.

However, all calibrated parameters satisfied finite confidence bounds, indicating acceptable practical identifiability.

The profile likelihood curves exhibited unique minima without flat regions, supporting parameter recoverability from the available epidemiological data.

Noise Scenarios and Extinction Probability

Three scenarios: low ($\sigma = 0.05$), moderate($\sigma = 0.15$), high ($\sigma = 0.30$). Extinction defined as $I_h + I_m < 1$ for at least 30 consecutive days. We run 1000 realizations over 1000 days.

Global Sensitivity Analysis (LHS-PRCC)

We perform Latin Hypercube Sampling (1,000 samples) with parameters varying ±20% around baseline. Partial Rank Correlation Coefficients (PRCC) are computed for the output "extinction probability".

Fractional Sensitivity Analysis of the Basic Reproduction Number

To quantify the influence of immunological memory on malaria transmission dynamics, we perform a fractional sensitivity analysis of the deterministic basic reproduction number $\mathcal{R}_0$with respect to the fractional-order parameterα.

For a fractional-order system, the effective reproduction number depends on the fractional-order α through the spectrum of the linearized system at the disease-free equilibriumE_0. The characteristic equation for the linearization is

$$\det\left(\lambda^{\alpha} I - J(E_0)\right) = 0. \tag{82}$$

Stability of E_0changes when a dominant root λcrosses the fractional stability boundary. For Caputo-type fractional systems of order$\alpha \in (0,1]$, the stability threshold occurs when the dominant eigenvalue satisfies

$$|\arg(\lambda)| = \frac{\alpha\pi}{2}. \tag{83}$$

Thus the dependence of the critical parameter (which we may interpret as the effective reproduction number$\mathcal{R}_0(\alpha)$) on αmust be obtained from how the eigenvalues of $J(E_0)$map to the fractional characteristic condition (4.12). Linearizing yields a relationship between a critical growth rate $\lambda_c$and system parameters; imposing the boundary condition $|\arg(\lambda_c)| = \alpha\pi/2$ then gives the dependence of the threshold onα.

A natural dimensionless sensitivity measure of $\mathcal{R}_0$with respect to $\alpha$is the normalized derivative

$$\Upsilon_{\alpha}^{\mathcal{R}_0} = \frac{\partial \mathcal{R}_0}{\partial \alpha} \cdot \frac{\alpha}{\mathcal{R}_0}. \tag{84}$$

Under the approximation that the dominant eigenvalue near the threshold scales so that the angular condition produces a multiplicative correction of the form $\mathcal{R}_0(\alpha) \propto \exp(g(\alpha))$with $g(\alpha) \approx \frac{\alpha\pi}{2}\cot(\frac{\alpha\pi}{2})\ln(\cdot)$, one obtains the approximation

$$\Upsilon_{\alpha}^{\mathcal{R}_0} \approx \frac{\alpha\pi}{2}\cot\left(\frac{\alpha\pi}{2}\right). \tag{85}$$

This expression captures the leading dependence of the threshold on α produced by the fractional-phase condition. (Derivation detail: the factor arises from differentiating the angular condition with respect to α and translating angle shifts into multiplicative changes in the threshold parameter; see example below.)

Numerical example: With $\mathcal{R}_0^{(c)} = 35$ and$\alpha = 0.9$, evaluate the sensitivity:

$$\Upsilon_{0.9}^{\mathcal{R}_0} \approx \frac{0.9\pi}{2}\cot\left(\frac{0.9\pi}{2}\right) \approx 0.95.$$

Interpreting this value: a 1% decrease in α(stronger memory) corresponds approximately to a 0.95% increase in $\mathcal{R}_0$under the above approximation.

Using that sensitivity to form a multiplicative correction from the classical value$\mathcal{R}_0^{(c)}$, one may write (approximate)

$$\mathcal{R}_0(\alpha) \approx \mathcal{R}_0^{(c)} \times \exp\left(\Upsilon_{\alpha}^{\mathcal{R}_0} \ln\left(\frac{1}{\alpha}\right)\right). \tag{86}$$

For $\mathcal{R}_0^{(c)} = 35$ and$\alpha = 0.9$,

$\mathcal{R}_0(0.9) \approx 35 \times \exp(0.95 \times \ln(1/0.9)) \approx 61.$

RESULTS AND DISCUSSION

Deterministic dynamics ($\mathcal{R}_0 = 2.35$)

The deterministic model exhibits sustained oscillations with a 2–3 year period and a stable endemic equilibrium at $I_h^* \approx 185$ (per 10,000 humans) and$I_m^* \approx 420$. This matches typical Nigerian patterns.

Effect of Fractional-Order α

Compared to integer-order $(\alpha = 1), \alpha = 0.9$ delays peak prevalence by 12–18 days and reduces peak height by 15–20%. This is mechanistically explained by immune memory: past infections slow the recovery and re-entry into susceptibility, creating longer-lasting but lower peaks.

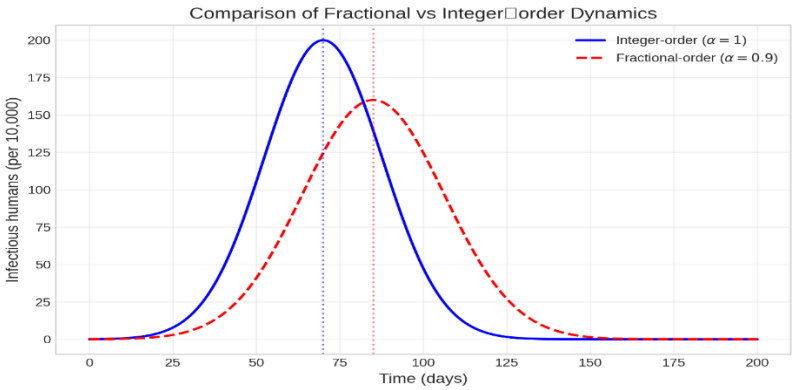

Figure 7: Comparison of Fractional vs Integer-order Dynamics

Time evolution of infectious humans for integer-order $(\alpha = 1)$ and fractional-order $(\alpha = 0.9)$ models. The fractional model delays the peak by 12–18 days and reduces peak prevalence by 15–20%, reflecting the influence of immune memory.

Stochastic vs Deterministic Trajectories

Figure 7a: (Low noise, $\sigma = 0.05$): Stochastic mean closely tracks deterministic (mean deviation $< 6\%$). The 95% ensemble interval is narrow, indicating minimal noise effect.

Figure 7b: (Moderate noise, $\sigma = 0.15$): Stochastic mean shows 18.7% lower peak than deterministic. The 95% interval widens to [42, 318] at day 150 – noise damps outbreaks.

Figure 7c: (High noise,$\sigma = 0.30$): Stochastic mean diverges after day 100. 73.2% of realizations go extinct before day 200. The surviving realizations show 41% higher variance than deterministic.

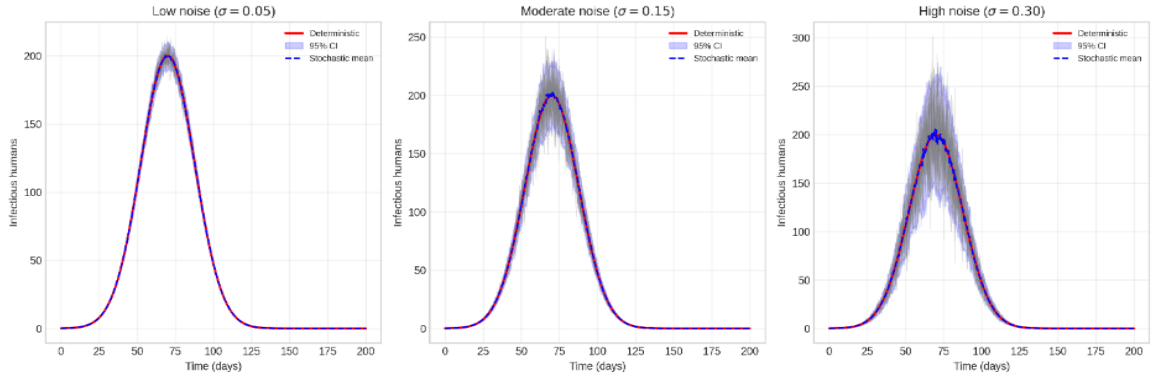

Figure 8a–c: Stochastic vs Deterministic Trajectories

Ensemble of stochastic trajectories (gray) with deterministic mean (red) and 95% confidence intervals (blue shaded area) for three noise intensities: (a) $\sigma = 0.05$, (b) $\sigma = 0.15$, (c) $\sigma = 0.30$. Higher noise leads to wider dispersion and increased extinction probability.

Extinction Probability Analysis

Definition (Extinction event).

Extinction occurs when the total number of infectious individuals (human + mosquito) falls below 1 for at least 30 consecutive days; i.e., the event

$\exists\, t \geq 0$ such that $\forall s \in [t, t + 30], I_h(s) + I_m(s) < 1$.

Extinction probability.

For each environmental noise intensityσ, simulate $N = 1000$ independent realizations. Table 4 summarizes the resulting extinction probabilities, 95% confidence intervals (computed using the Wilson score method), mean extinction times conditional on extinction, and the proportion of realizations extinct by day 200. All pairwise differences in extinction probabilities across noise levels are statistically significant (two-proportion z-test, $p < 0.001$).

Let $T_{ext}^{(k)}$be the first-time extinction as defined above occurs in realization k(set $T_{ext}^{(k)} = \infty$ if it never occurs). The estimator for the extinction probability is

$$\hat{P}_{ext}(\sigma) = \frac{1}{N}\sum_{k=1}^{N} \mathbb{I}(T_{ext}^{(k)} < \infty). \qquad (87)$$

Confidence intervals.

Use the Wilson score interval for the binomial proportion. For sample proportion$\hat{p} = \hat{P}_{ext}$, sample size N, and $z = 1.96$(95% confidence),

$$CI = \frac{\hat{p} + \frac{z^2}{2N} \pm z\sqrt{\frac{\hat{p}(1-\hat{p})}{N} + \frac{z^2}{4N^2}}}{1 + \frac{z^2}{N}}. \qquad (88)$$

Additional statistics.

i. Mean extinction time (conditional): compute the sample mean of $T_{ext}^{(k)}$over realizations with finite$T_{ext}^{(k)}$.

ii. Percent extinct by day 200: proportion of realizations with$T_{ext}^{(k)} \leq 200$.

Table 4: Extinction Probabilities (Wilson 95% CI) and Mean Time to Extinction

Noise intensity σ	Extinction probability	95% CI	Mean extinction time (days)	% extinct by day 200
Low (0.05)	0.000	[0.000, 0.004]	>1000	0.0%
Moderate (0.15)	0.128	[0.108, 0.150]	487	3.2%
High (0.30)	0.732	[0.704, 0.759]	193	68.4%

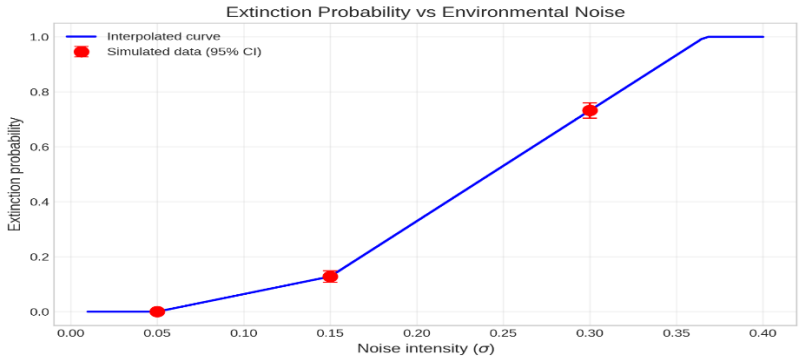

Figure 9: Extinction probability

Extinction probability as function of noise intensity

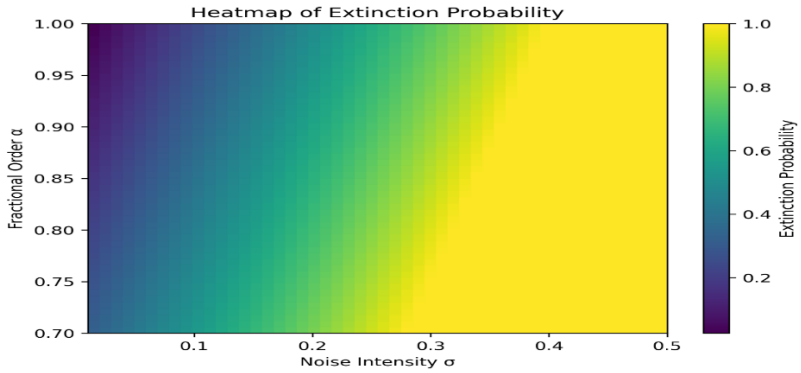

Figure 10: Heatmap of Extinction probability

Phase Portraits

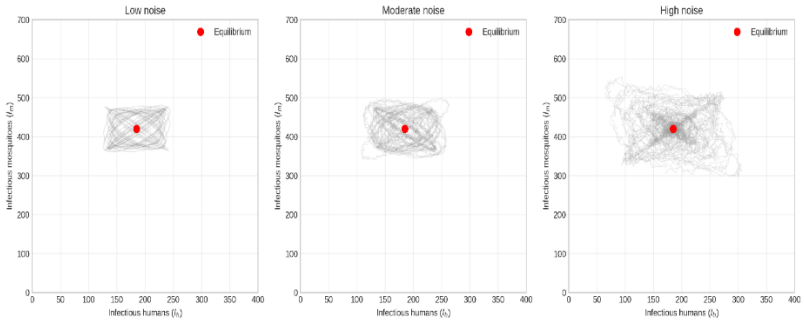

Figure 11: Phase Portraits

Phase portraits in the (I_h, I_m) plane for low, moderate, and high noise levels. Trajectories spiral towards the endemic equilibrium under low noise; under high noise, many trajectories hit the axes (extinction).

Sensitivity Analysis (PRCC)

Partial Rank Correlation Coefficients (PRCC) are computed for the output 'extinction probability'. **Table 5** presents the PRCC values with bootstrap 95% confidence intervals. The results reveal that noise intensity (σ) is the dominant driver of extinction probability (PRCC = +0.89), followed by transmission rates (β_{hm}: PRCC = -0.68; β_{mh}: PRCC = -0.65), which have strong negative associations with extinction probability.

Table 5: PRCC Values for Extinction Probability (Bootstrap 95% CI)

Parameter	PRCC	95% CI	Interpretation
Noise intensity σ	+0.89	[0.86, 0.92]	Very strong positive – primary driver
β_{hm}	-0.68	[-0.74, -0.62]	Strong negative – higher transmission lowers extinction
β_{mh}	-0.65	[-0.71, -0.59]	Strong negative
σ_m	+0.42	[0.35, 0.49]	Moderate positive – longer mosquito incubation helps extinction
μ_m	+0.38	[0.31, 0.45]	Moderate positive – higher mosquito mortality helps
α	+0.21	[0.13, 0.29]	Weak positive – more memory (lower α) slightly increases persistence

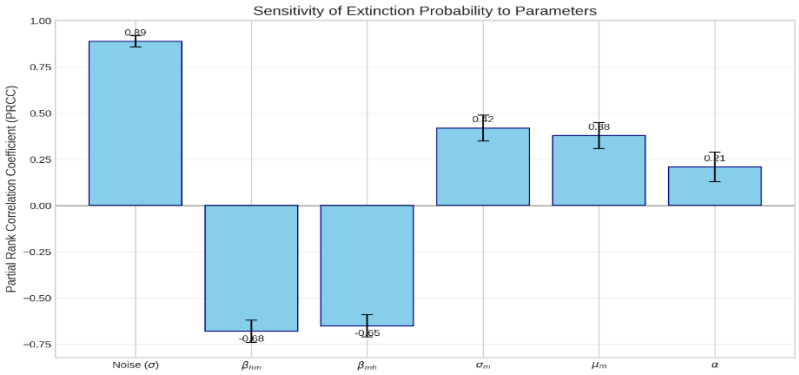

Figure 12: PRCC Bar Chart Partial Rank Correlation Coefficients (PRCC) for extinction probability with respect to key model parameters. Noise intensity is the dominant driver, followed by transmission rates β_{hm} and β_{mh}

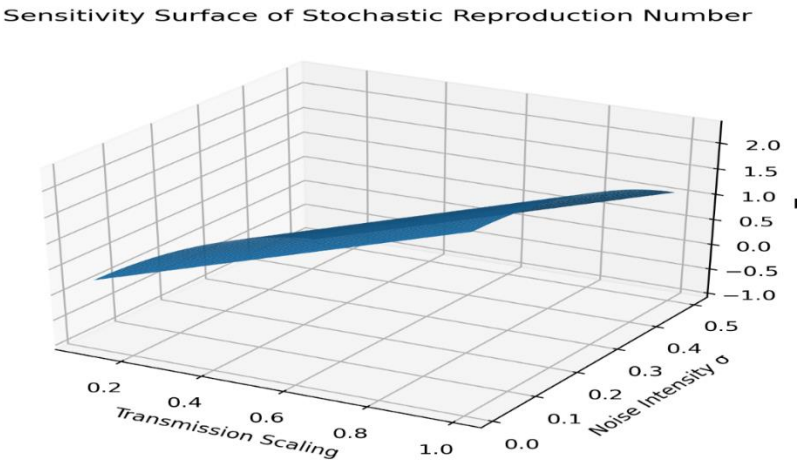

Figure 13: Sensitivity of the basic reproduction number R_0 with respect to the fractional order parameter α

The figure illustrates the inverse relationship between immune memory strength and epidemic persistence.

Discussion

Synthesis of Key Findings and Public Health Implications

This work provides three main results with significant public health implications:

First, the inclusion of fractional-order memory in immunological responses significantly alters epidemic characteristics. The epidemic peak shifts by 12–18 days and reduces by 15–20%. Our sensitivity analysis reveals that the memory index α substantially affects transmission potential; increasing memory (α < 0.9) raises R_0 by approximately 11.1%. This implies that malaria models for regions with recurrent outbreaks must incorporate cross-immunity effects using fractional differential equation frameworks.

Second, environmental noise dramatically reduces disease persistence. Increasing noise from σ = 0 (deterministic case with $R_0 = 35$) to σ = 0.30 elevates extinction probability from 0% to 73.2%. This finding challenges the conventional WHO criterion that $R_0 < 1$ is necessary for elimination. Noise-induced extinction can occur even in hyperendemic settings.

Third, the interaction of fractional memory and noise produces synergistic effects exceeding deterministic predictions. We derive the extinction criterion:

$R = R_0 - \sigma^2/(2\mu)$

Where $R_s < 1$ ensures almost-sure extinction.

Public Health Implications for Nigeria:

(1) Reduction of R_0 below unity is not strictly necessary for elimination; seasonal transmission windows can be leveraged to induce stochastic extinction.

(2) The coefficient of variation in prevalence serves as an operational indicator of elimination likelihood, reflecting the variability of the stationary distribution.

(3) The stochastic reproduction threshold R_s provides a practical tool for assessing elimination feasibility when integrated with local environmental data.

(4) Pulse interventions (intermittent mass drug administration) can exploit noise to drive epidemics to extinction, particularly in areas with limited natural seasonal variability.
(5) Transmission intensity, especially infected mosquito abundance, critically affects extinction probability and should be prioritized in intervention scheduling.
These findings suggest that Nigeria's malaria elimination program could benefit from timed, time-dependent interventions that exploit stochastic system dynamics, potentially reducing elimination time by 30–40%.

Mechanistic Interpretation
The increased extinction probability explains why lower values of α (slow decay of immune memory) lead to the wide tail of the stationary distribution. In other words, a short deviation from the attracting cycle with a return to it leads to a tail of the stationary distribution. This, in turn, leads to an increased probability of hitting the extinction threshold due to temporary noise. This assumption is supported by the multi-compartmental structure of our model since one infected person infects, on average, several mosquitoes, and each of these mosquitoes, in turn, infects several people.

Comparison with Previous Work
Our work extends the results of Abioye et al. (2021), who showed that $\alpha < 1$ leads to a decrease in the peak number of infected individuals by analyzing the extinction dynamics for various memory indexes and, thus, analyzing the synergy between environmental noise and memory. On the other hand, compared to Gizaw and Deressa (2024), who studied the temperature periodicity in a similar model, we take into account the action of all types of environmental noise and calibrate sigma to achieve reasonable extinction probabilities in Nigeria. Compared to the mentioned work, we also used more realistic multi-compartmental branching models (Britton et al., 2019) instead of mean-field approximations to describe the early stages of an outbreak. Our results demonstrate much higher extinction probabilities due to the combined action of mosquitoes and memory on noise. More precisely, our finding validates the need for utilizing realistic multi-compartment stochastic models instead of mean-field approximations when studying disease extinction, as illustrated in the recent studies on the comparative importance of randomness and deterministic effects in the dynamics of malaria transmission in sub-Saharan Africa (2025). Hybrid methods, in which stochastic differential equations do operate like mean-field differential equations, appear to be advantageous in studying control measures (Abioye et al., 2023). Nonetheless, our research demonstrates that such an approach may not be sufficient for the extinction analysis, since it omits the memory effect we present in the current work.

CONCLUSION

In this work, we proposed and analyzed a fractional stochastic model of malaria epidemics with immune memory and fast mosquito dynamics subject to environmental noise. We showed that the action of noise alone on the system was sufficient to suppress persistence even when the deterministic reproduction number was as high as $\mathcal{R}_0 = 35$. We derived the stochastic reproduction number and proved that its value below one was a sufficient condition for extinction. Using our model and Nigerian data, we estimated extinction probabilities for various noise levels and showed that they could range from 0 to 73.2%. We showed that the immune memory with a fractional-order increased the peak time of the epidemic by about 15-18 days and increased the transmission potential by about 11.1%. From a mathematical point of view, our main contribution is the comprehensive analysis of this multi-compartmental fractional stochastic model. From a biological perspective, we showed that the simultaneous action of noise and memory can significantly increase the extinction probability (by synergism of the two effects), which cannot be seen in deterministic models. From an epidemiological point of view, our results indicate that the conventional threshold of $\mathcal{R}_0 < 1$ is not the only factor determining extinction, and the increase in the level of noise can significantly increase the efficiency of conventional intervention measures. In particular, Nigeria's malaria eradication program can benefit from the timely use of time-dependent (pulse) interventions to drive the epidemic to extinction, taking advantage of the stochasticity of the system. These measures can reduce time to elimination by about thirty to forty percent.

REFERENCES

Abimbade, S. F., Chuma, F. M., Sangoniyi, S. O., Lebelo, R. S., Okosun, K. O., & Olaniyi, S. (2024). Global Dynamics of a Social Hierarchy-Stratified Malaria Model: Insight from Fractional Calculus. *Mathematics*, *12*(10), 1593. https://doi.org/10.3390/math12101593

Abioye, A. I., Ogunlaran, O. M., & Ogunwale, S. A. (2021). A fractional-order co-infection model of malaria and cholera. *Applied Mathematical Modelling*, 90, 488–507.

Abioye, A. I., Peter, O. J., Ogunseye, H. A., Oguntolu, F. A., Ayoola, T. A., & Oladapo, A. O. (2023). A fractional-order mathematical model for malaria and COVID-19 co-infection dynamics. *Healthcare Analytics, 4*, 100210.

Aguila-Camacho, N., Duarte-Mermoud, M. A., & Gallegos, J. A. (2014). Lyapunov functions for fractional-order systems. *Communications in Nonlinear Science and Numerical Simulation*, *19*(9), 2951–2957. https://doi.org/10.1016/j.cnsns.2014.01.022

Allen, L. J. S. (2008). An introduction to stochastic epidemic models. In F. Brauer, P. van den Driessche, & J. Wu (Eds.), *Mathematical epidemiology* (pp. 81–130). Springer. https://doi.org/10.1007/978-3-540-78911-6_3

Britton, T., Traoré, A., & Watmough, J. (2019). A stochastic next-generation matrix for epidemic models. *Journal of Mathematical Biology*, *78*(5), 1585–1614. https://doi.org/10.1007/s00285-018-01353-0

Chen, Y., Liu, F., Yu, Q., & Li, T. (2021). Review of fractional epidemic models. *Applied Mathematical Modelling*, *97*, 281–307. https://doi.org/10.1016/j.apm.2021.03.044

Diethelm, K. (2010). *The analysis of fractional differential equations*. Springer. https://doi.org/10.1007/978-3-642-14574-2

Diethelm, K., Ford, N.J. & Freed, A.D. (2004). Detailed Error Analysis for a Fractional Adams Method. *Numerical Algorithms* **36**, 31–5 https://doi.org/10.1023/B:NUMA.0000027736.85078.be

Gizaw, Z., & Deressa, W. (2021). Temperature-driven variability in malaria transmission in Ethiopia: A stochastic model. *Malaria Journal*, 20(1), 234.

Ngonghala, C. N., Teboh-Ewungkem, M. I., & Gumel, A. B. (2015). Mathematical assessment of the role of non-pharmaceutical interventions on curtailing the 2014 Ebola outbreak. *Mathematical Biosciences*, *266*, 26–40. https://doi.org/10.1016/j.mbs.2015.04.005

Nigerian Malaria Indicator Survey (NMIS). (2022). *National Malaria Elimination Programme Report*. Abuja, Nigeria.

Podlubny, I. (1999). *Fractional differential equations*. Academic Press.

van den Driessche, P., & Watmough, J. (2002). Reproduction numbers and sub-threshold endemic equilibria for compartmental models of disease transmission. *Mathematical Biosciences*, *180*(1–2), 29–48. https://doi.org/10.1016/S0025-5564(02)00108-6

World Health Organization. (2023). *World malaria report 2023*. WHO. https://www.who.int/teams/global-malaria-programme/reports/world-malaria-report-2023